

# Identification of beam crack using the dynamic response of a moving spring-mass unit

Ning An\*, He Xia and Jiawang Zhan

*School of Civil Engineering, Beijing Jiaotong University, Beijing 10004, China*

(Received July 26, 2010, Accepted October 22, 2010)

**Abstract.** A new technique is proposed for bridge structural damage detection based on spatial wavelet analysis of the time history obtained from vehicle body moving over the bridge, which is different from traditional detection techniques based on the bridge response. A simply-supported Bernoulli-Euler beam subjected to a moving spring-mass unit is established, with the crack in the beam simulated by modeling the cracked section as a rotational spring connecting two undamaged beam segments, and the equations of motion for the system is derived. By using the transfer matrix method, the natural frequencies and mode shapes of the cracked beam are determined. The responses of the beam and the moving spring-mass unit are obtained by modal decomposition theory. The continuous wavelet transform is calculated on the displacement time histories of the sprung-mass. The case study result shows that the damage location can be accurately determined and the method is effective.

**Keywords:** moving load; beam; dynamic response; damage detection; wavelet transform; Lipschitz exponent.

---

## 1. Introduction

The vibration of cracked structures has been researched for decades. There are basically two crack models: 1) reducing stiffness in a finite element (Bamnnio 2002, Sinha 2002), 2) using a rotational spring to represent the cracked section (Yuen 1985). The second model, combined with fracture mechanics, has been most popular amongst the researchers. The dynamic behavior of a cracked, simply supported uniform beam was studied and the crack was simulated by an equivalent spring, connecting the two segments of the beam (Narkis 1994, Narkis and Elmalah 1996). It is found that the only information required for accurate crack identification is the variation of the first two natural frequencies due to the crack. The coupling effect between the crack depth and the axial load on the natural frequency of a prestressed fixed-fixed beam was investigated and the experimental work verified the results of the theoretical analysis (Masoud *et al.* 1998). The study shows that there is a significant coupling between the axial load and crack depth, and this coupling effect is directly proportional to the crack depth as well as the axial load. An iterative modal analysis approach was developed to determine the effect of transverse cracks on the dynamic behavior of simply supported undamped Bernoulli–Euler beams subject to a moving mass (Mahmoud 2002). Xiang and Zhang (2009) presented an analytic solution of the modal properties of simply-supported Euler-Bernoulli

---

\* Corresponding author, Doctoral Student, E-mail: AnNing1205@163.com

beams that contain a general damage with no additional assumptions, where the damage can be a reduction in the bending stiffness or a loss of mass within a beam segment. The study shows that the lower natural frequencies and mode shapes do not change so much when a section of the beam is damaged, while the mode of rotation angle and curvature modes show abrupt change near the damaged region. Philip (2009) established a new model which uses modified an energy function to account for molecular interactions in the vicinity of crack tips, resulting in Barenblatt cohesive forces. The model shows that local minimization is necessary to yield a physically reasonable result.

The exact effect of crack and mass depends on the speed, time, crack size, crack location, and the moving mass level. A theoretical and experimental study of the response of a damaged Euler–Bernoulli beam traversed by a moving mass was presented by Bilello (2004). It is shown that experimental results are in good agreement with the theoretical predictions.

As the inverse problem of above, the damage identification in civil engineering structures is also a considerable attention from researchers in the last two decades (Salawu 1997, Doebling *et al.* 1998, Montalvão *et al.* 2006). The wavelet-based crack detection method is one of the non-model-based methods (Staszecski 1998). Wavelet functions are composed of a family of basic functions that are capable of describing a signal in both the localized time (or space) domain and the frequency (or scale) domain (Daubechies 1992). Wavelet analysis can reveal some hidden aspects of the data that traditional Fourier analysis fails to detect. This property is particularly important for damage detection applications. The continuous wavelet transform of the fundamental mode shape and its Lipschitz exponent was used to detect the damage location and extent in a beam by Hong *et al.* (2002), Gentile and Messina (2003), Douka *et al.* (2003), Loutridis *et al.* (2005) and Han *et al.* (2005). However, it is very difficult to obtain accurate mode shape in practice and the differentiation of the mode shape may further amplify the measurement error. Thus a new method for crack identification of bridge beam based on wavelet analysis is proposed, in which the continuous wavelet transform of the deflections of the bridge deck subject to moving vehicular loads and its Lipschitz exponent is used to detect the damage location and extent in a beam (Zhu and Law 2006).

In this paper, the dynamic response of a vehicle is studied when it moves cross a cracked bridge, which was studied rarely in the past, and the response is analyzed using the continuous wavelet transform. In the simulation, the vehicle is modeled as a moving spring-mass unit, and the bridge is simplified as an Euler–Bernoulli beam simply-supported at both ends. The influence of the vehicle-bridge interaction system parameters on the damage detection is investigated.

## 2. Dynamic model of cracked beam under moving spring-mass unit

Shown in Fig. 1 is the model of the bridge–vehicle system. The bridge is assumed to be a simple-supported Euler–Bernoulli beam with constant cross-section and constant mass along its length. The moving vehicle is idealized by a spring-mass unit with two degrees-of-freedom.  $M_1$  and  $M_2$  denote the unsprung and sprung-mass, respectively, and the wheel contact is assumed to be at single point only. The vehicle moves at constant speed  $v$ , from left to right. The equations of motion of the system can be expressed as

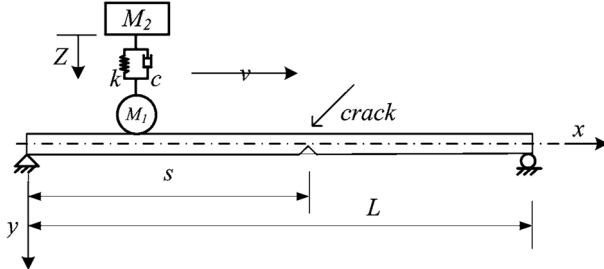


Fig. 1 A simply-supported beam with crack subject to moving spring-mass unit

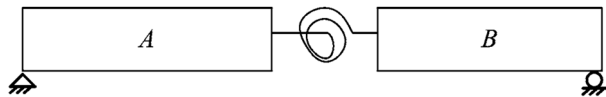


Fig. 2 Beam with rotational springs representing damaged section

$$\begin{cases} EI \frac{\partial^4 y(x, t)}{\partial x^4} + \rho A \frac{\partial^2 y(x, t)}{\partial t^2} + c_b \frac{\partial y(x, t)}{\partial t} = \delta(x - vt)P(x, t) \\ M_2 \ddot{Z}(t) + c[\dot{Z}(t) - \dot{y}(x, t)|_{x=v t}] + k[Z(t) - y(x, t)|_{x=v t}] = 0 \end{cases} \quad (1)$$

where;  $P(x, t) = (M_1 + M_2)g - M_1 \frac{\partial^2 y(x, t)}{\partial t^2} - M_2 \ddot{Z}(t)$ ;  $y$ ,  $EI$ ,  $\rho A$  and  $c_b$  are deflection, flexural rigidity, mass per unit length and damping of the beam;  $Z$  is the displacement of the sprung-mass  $M_2$ ;  $k$  and  $c$  are spring stiffness and damping coefficient, respectively. The unsprung-mass  $M_1$  is idealized by a single mass point and is in indirect contact with the beam.

The crack is a single-sided crack which does not change the mass of the beam. The cracked section is modeled as a rotational spring connecting two undamaged beam segments, as shown in Fig. 2. The stiffness of the rotational spring  $k_c$  is determined by using fracture mechanics. It is given the angle of rotation of a uniform strip with an edge crack under pure bending moment  $C = 1/k_c$  (Tada 1973). For a rectangular section of height  $H$  with a crack of depth  $h$ ,  $C$  can be expressed as

$$C = \frac{2H}{EI} \left( \frac{h/H}{1-h/H} \right)^2 [5.93 - 19.69 h/H + 37.14(h/H)^2 - 35.84(h/H)^3 + 13.12(h/H)^4] \quad (2)$$

where:  $h/H$  is the normalized crack depth, the ratio of crack depth to section height.

The vertical displacement of the beam can be written as

$$y(x, t) = \phi(x)q(t) \quad (3)$$

where:  $q(t)$  is the generalized displacement;  $\phi(x)$  is the mode shape function, which can be written as

$$\phi(x) = \begin{cases} \phi_A(x) = A_1 \sin(ax) + B_1 \cos(ax) + C_1 \sinh(ax) + D_1 \cosh(ax) & (0 \leq x < s) \\ \phi_B(x) = A_2 \sin(ax) + B_2 \cos(ax) + C_2 \sinh(ax) + D_2 \cosh(ax) & (s \leq x \leq L) \end{cases} \quad (4)$$

where  $\phi_A(x)$  and  $\phi_B(x)$  are respectively the modal functions of Segment A and Segment B,  $a^4 = \omega^2 \rho A^4 / EI$ .

The boundary conditions are

$$\begin{cases} \phi_A(0) = 0 & \phi_A(s) = \phi_B(s) \\ \phi'_A(0) = 0 & \phi'_A(s) = \phi'_B(s) - CEI\phi''_B(s) \\ \phi_B(L) = 0 & \phi''_A(s) = \phi''_B(s) \\ \phi''_B(L) = 0 & \phi'''_A(s) = \phi'''_B(s) \end{cases} \quad (5)$$

where  $L$  and  $s$  are respectively the span of the beam and the distance from the left-hand end to the crack section.

Substituting these boundary conditions into Eq. (4) yields a system of linear homogeneous algebraic equations with eight unknowns:  $A_i$ ,  $B_i$ ,  $C_i$ ,  $D_i$  ( $i = 1, 2$ ). For a nontrivial solution, the determinant of the coefficient of these equations must equal to 0 for each  $a$ , shown as Eq. (6).

$$\begin{bmatrix} 0 & 1 & 0 & 1 & 0 & 0 & 0 & 0 \\ 0 & -1 & 0 & 1 & 0 & 0 & 0 & 0 \\ 0 & 0 & 0 & 0 & s_1 & c_1 & sh_1 & ch_1 \\ 0 & 0 & 0 & 0 & -s_1 & -c_1 & sh_1 & ch_1 \\ s_2 & 0 & sh_2 & 0 & -s_2 & -c_2 & -sh_2 & -ch_2 \\ c_2 - \eta s_2 & 0 & ch_2 + \eta sh_2 & 0 & -c_2 & s_2 & -ch_2 & -sh_2 \\ -s_2 & 0 & sh_2 & 0 & s_2 & c_2 & -sh_2 & -ch_2 \\ -c_2 & 0 & ch_2 & 0 & c_2 & -s_2 & -ch_2 & -sh_2 \end{bmatrix} = 0 \quad (6)$$

where  $s_1 = \sin(aL)$ ,  $c_1 = \cos(aL)$ ,  $sh_1 = \sinh(aL)$ ,  $ch_1 = \cosh(aL)$ ,  $s_2 = \sin(as)$ ,  $c_2 = \cos(as)$ ,  $sh_2 = \sin(as)$ ,  $ch_2 = \cosh(as)$  and  $\eta = CEIa$ .

Using the equation,  $A_i$ ,  $B_i$ ,  $C_i$  and  $D_i$  ( $i = 1, 2$ ) can be determined, and then  $\phi(x)$  can be readily solved from Eq. (4). Substituting Eq. (3) into Eq. (1), the dynamic responses of the beam and sprung-mass can be obtained.

### 3. Crack identification using continuous wavelet transform

The continuous wavelet transform of a square-integrable signal  $f(x)$ , where  $x$  is time or space, is defined as (Mallat and Hwang 1992)

$$Wf(u, s) = f(x) \otimes \psi_s(x) = \frac{1}{\sqrt{s}} \int_{-\infty}^{\infty} f(x) \psi^* \left( \frac{x-u}{s} \right) dx \quad (7)$$

where:  $\otimes$  denotes the convolution of two functions;  $\psi_s(x)$  is the dilation of  $\psi(x)$  by the scale factor  $s$  and translation factor  $u$ ;  $\psi^*(x)$  is the complex conjugate of  $\psi(x)$  which is a mother wavelet and usually called the Mexican Hat wavelet that has the following explicit expression

$$\psi(x) = \frac{d^2 \theta}{dx^2} = \frac{2}{\sqrt{3}\sigma} \pi^{-1/4} \left( \frac{x^2}{\sigma^2} - 1 \right) \exp \left( -\frac{x^2}{2\sigma^2} \right) \quad (8)$$

where  $\theta(x)$  is the Gaussian function,  $\sigma$  is the standard deviation.

The Mexican Hat wavelet is second-order differential of the Gaussian function which is smooth. So the wavelet transform can be used to replace the direct differentiation of the displacement to get the curvature properties. The second differential of the displacement time history of a beam is not continuous at the damage location, while the displacement time history is continuous. The damage can then be located using the wavelet transform of the displacement time history when the beam is subject to the moving load. And the crack depth can be characterized by the Lipschitz exponent  $\alpha$ .

#### 4. Numerical examples

A simply-supported beam with a 50 m length, and a 1.0 m height and 0.5 m width section is used. The Young's modulus and density of the beam are respectively  $E = 2.1 \times 10^{11}$  Pa and  $\rho = 7860$  kg/m<sup>3</sup>, and the damping ratio for all modes is taken as 0.02. The first four natural frequencies are thus calculated to be 5.89 Hz, 23.56 Hz, 53.02 Hz and 94.25 Hz. The unsprung and sprung-masses are 5t and 35t, respectively. The stiffness of spring is  $1.5 \times 10^6$  kN/m and the damping is 160 kNs/m.

##### 4.1 Crack effect on the frequencies of beam

A crack in the beam may decrease the stiffness, reduces the natural frequencies and affects the mode shapes. The frequencies of the beam are the function of the depth and location of the crack, as

$$\omega_i / \omega_i^0 = f(s/L, h/H) \quad (9)$$

where,  $s$  is the distance of the crack position to the left support of the beam,  $h/H$  is the normalized crack depth,  $\omega_i^0$  is the  $i$ th frequency of the uncracked beam, and the  $i$ th frequency of the cracked beam can be written as  $\omega_i = a^2 \sqrt{EI/\rho A}$ , where  $a$  can be determined from Eq. (6).

The normalized crack location  $s/L$  is from 0 to 1, and the normalized crack depth  $h/H$  from 0 to 0.5. The calculated results are shown in Fig. 3.

As shown in the figure, the frequencies of the beam change obviously when the crack occurs at the location where the absolute value of mode shape is high, while change less obviously when the crack occurs at the stationary point of mode shape. The frequencies do not change much when the crack is not deep ( $h/H < 0.3$ ), when the crack depth ratio reaches 30%, the first four frequencies all decreased by 2.3% at most; and when the depth ratio reaches 50%, the 1st frequency decreased by 10.5% at most, the 2nd 9.5%, the 3rd 9% and the 4th 8%, respectively.

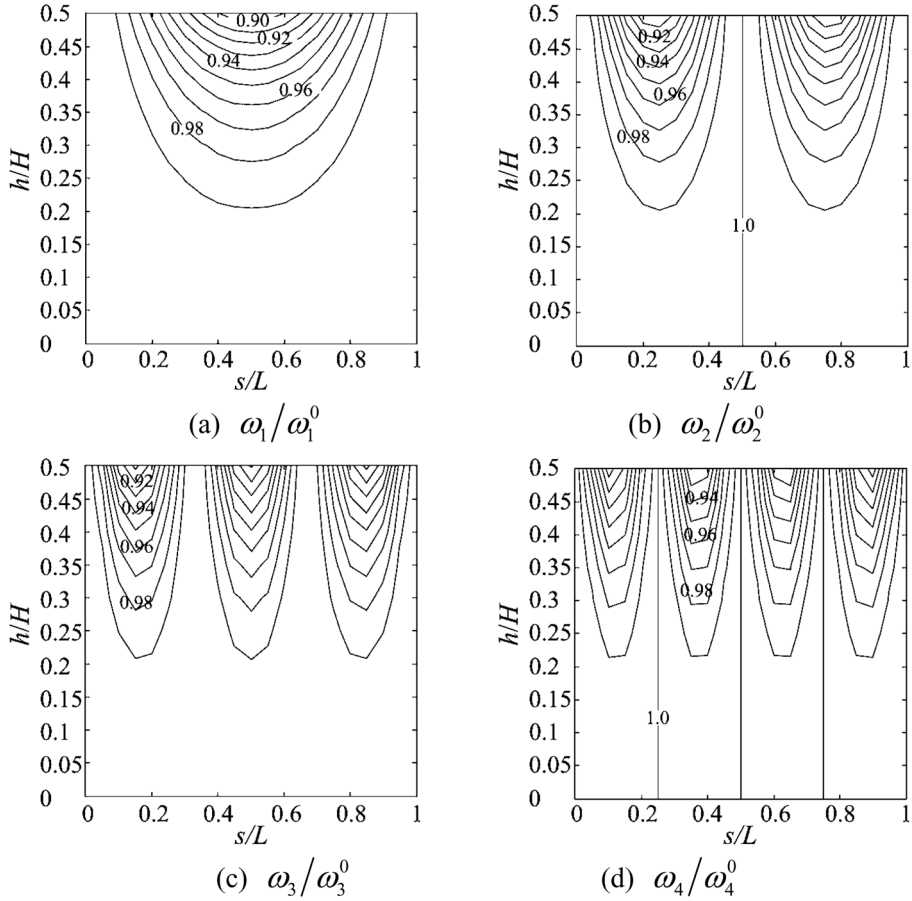


Fig. 3 Frequency ratios corresponding to different crack depth and location ratios

#### 4.2 Crack effect on the responses of beam and sprung-mass

The presence of crack changes the response of the beam to moving loads. Eq. (1) is used to obtain the dynamic response of the simple beam subjected to a moving spring-mass unit. In this case, the speed is 20 m/s;  $h/H$  is 0, 0.2, 0.3 and 0.4, respectively. The time step is  $L/500v$  in calculation. Substituting Eq. (3) into Eq. (1), the dynamic responses of the beam and the sprung mass can be calculated.

As shown in Fig. 4, when the crack locates at  $s = 0.3L$ , the vertical deflection of the beam and the vertical displacement of the sprung mass become larger with the increase of crack depth, while the shapes of response curves change little. The changing rate of sprung-mass displacement is approximately equal to that of the beam.

#### 4.3 Damage location identification

The continuous wavelet transform on the time history of the sprung-mass displacement is calculated.

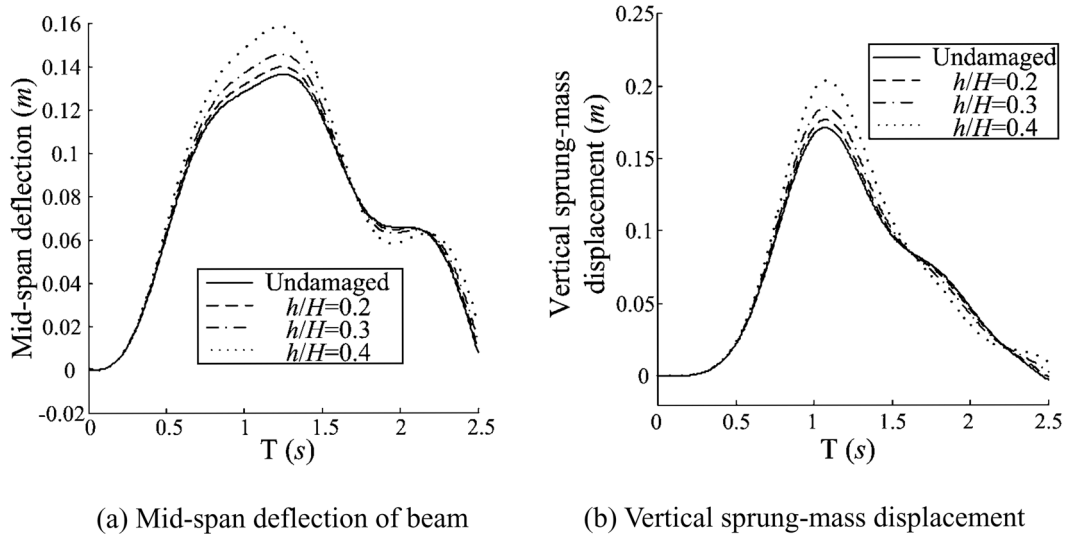
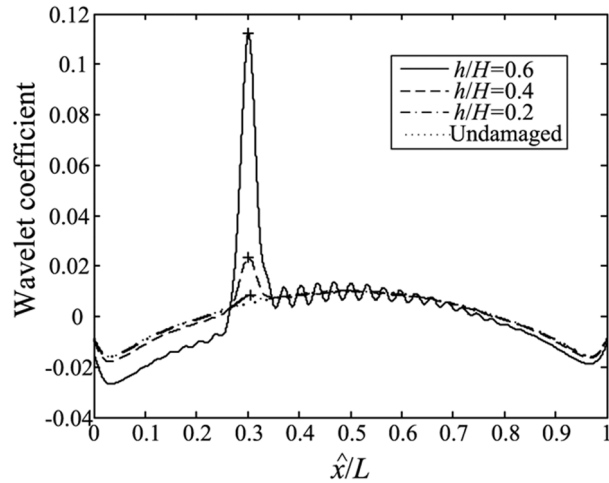
Fig. 4 Dynamic responses ( $s/L=0.3$ )Fig. 5 Wavelet coefficients ( $scale = 82$ )

Fig. 5 shows the wavelet coefficients of the sprung-mass displacement with scale 82 when the crack is at  $0.3L$  and the depth ratios are 0, 0.2, 0.4 or 0.6. The moving speed is 1 m/s. Both the unsprung- and sprung-masses are 40t. The spring stiffness is 1500 kN/m. It can be seen that the crack location is identified accurately. The location is identified as the position of the maximum value in the wavelet coefficient curve. The maximum value in the curve becomes larger when the crack depth increases, but the identified location does not change.

Fig. 6 shows the identified location of the crack using different scales. The identified location is close to  $0.3 L$  when the scale is between 54 and 296 ( $|\hat{x} - x|/L \leq 0.05$ ), while it is close to the two ends when the scale is less than 54, which is associated with the discontinuity of the measured responses on the entrance and exit of the moving load, and a little far from the crack

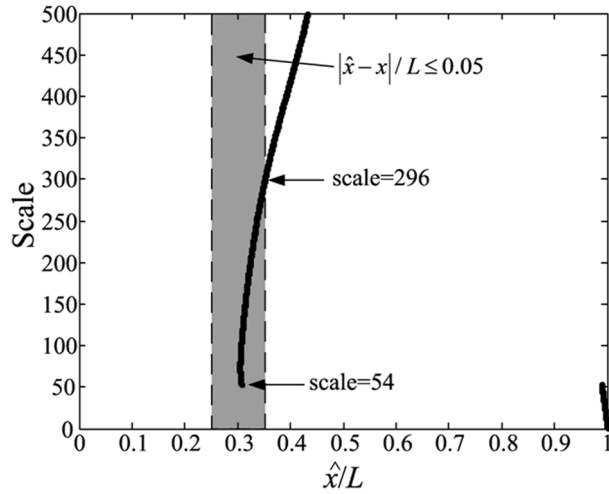


Fig. 6 Identified crack location using different scales

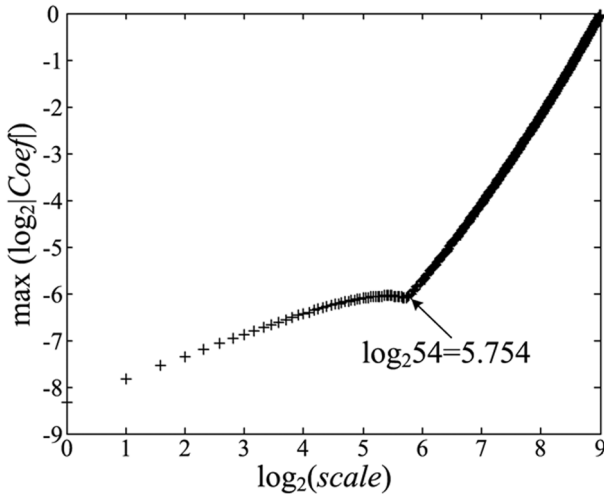


Fig. 7 Logarithm value of maximum wavelet coefficients using different scales

( $|\hat{x} - x|/L > 0.05$ ) when the scale is larger than 296.

The maximum value of wavelet coefficient is plotted versus the scale in a log-log plot in Fig. 7. When the scale is larger than 54, the curve becomes approximately a straight line.

$$\log_2 |Wf(u_d, s)| = \log_2 |K| + \alpha \log_2 |scale| \quad (9)$$

The slope  $\alpha$  is called the Lipschitz exponent, that changes when the crack extent changes. So the Lipschitz exponent  $\alpha$  is defined to express the crack extent.

Table 1 shows the Lipschitz exponent  $\alpha$  defined by Eq. (10) for cracks with different depth at different location. The  $\alpha$  decreases with the increase of crack depth. The corresponding relationship between  $\alpha$  and crack depth can be determined for a beam as a database for assessment of particular crack damage in future measurements.

Table 1  $\alpha$  with different depth and location

Crack location	Crack depth ratio				
	0.1	0.2	0.3	0.4	0.5
0.3 $L$	2.3971	2.2225	2.0071	1.7852	1.6653
0.5 $L$	2.4659	2.3532	2.1925	2.0411	1.8471
0.7 $L$	2.4598	2.3386	2.1715	1.9907	1.8051

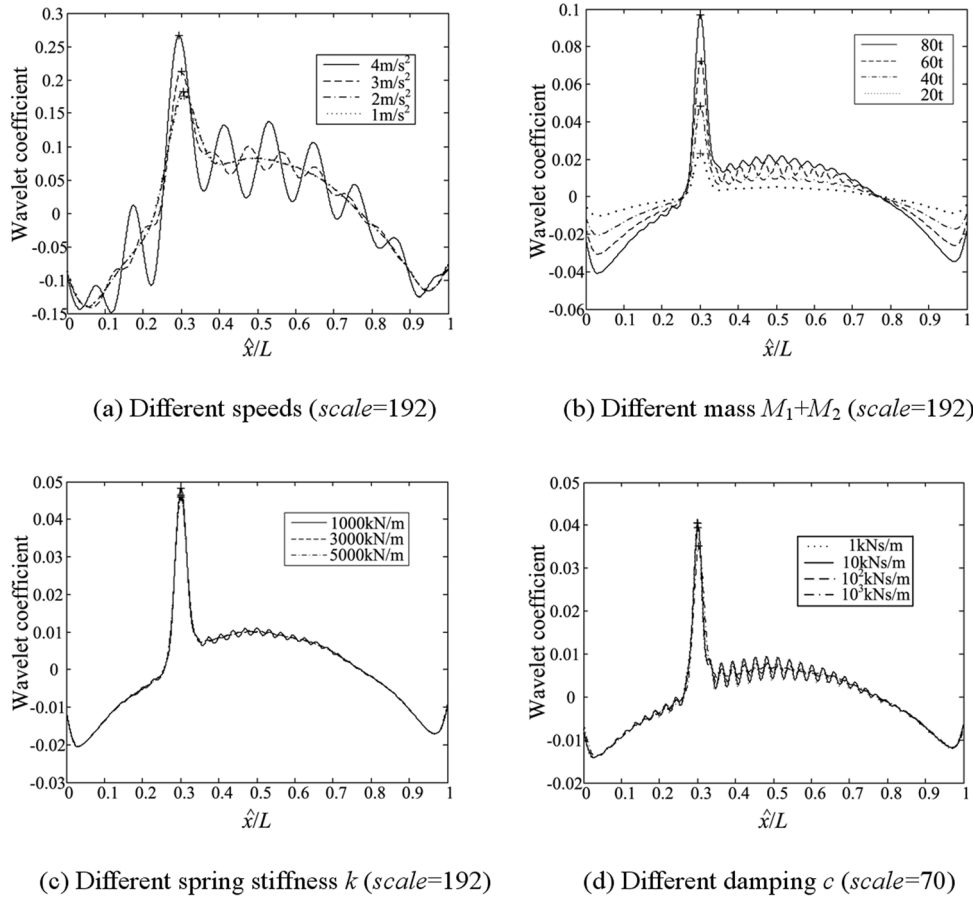


Fig. 8 Wavelet coefficients with different parameters

Shown in Fig. 8 are the wavelet coefficients of sprung-mass displacement with different parameters, when the crack is at  $0.3L$  and the crack depth ratio is 0.5.

Fig. 8(a) shows the wavelet coefficients with scale 192 when the load is moving on the beam at different speeds (1 m/s, 2 m/s, 3 m/s or 4 m/s), where the unsprung and sprung-masses are both 40 t, the spring stiffness is 1500 kN/m, and the damping is  $10^4$  kNs/m.

Fig. 8(b) shows the wavelet coefficients with scale 192 when the unsprung- and sprung-masses are both simultaneously changed as 20 t, 40 t, 60 t and 80 t, where the moving speed is 1 m/s, the spring stiffness 1500 kN/m, and the damping is  $10^4$  kNs/m.

Fig. 8(c) shows the wavelet coefficients with scale 192 when the spring stiffness is changed as 1000 kN/m, 3000 kN/m and 5000 kN/m, where the moving speed is 1 m/s, the unsprung- and sprung-masses are both 40 t, and the damping is  $10^4$  kNs/m.

Fig. 8(d) shows the wavelet coefficients with scale 70 when the damping is changed as 1 kNs/m, 10 kNs/m, 100 kNs/m and 1000 kNs/m, where the moving speed is 1 m/s, the unsprung- and sprung-masses are both 40 t, and the spring stiffness is 1500 kN/m.

From the figures one can see that the position of the maximum value does not obviously change with the variation of unsprung and sprung-masses, spring stiffness and damping, but can be identified more clearly when the load speed is lower. The maximum value of the wavelet coefficient becomes bigger with increase of load speed and the unsprung- and sprung-masses, but change little with the variation of spring stiffness and damping.

## 6. Conclusions

The effect of crack on the dynamic behavior of simply-supported undamped Bernoulli- Euler beams subject to a moving spring-mass unit is studied.

A new method for bridge structural damage detection is proposed based on spatial wavelet analysis of the time history of sprung-mass of a spring-mass unit which is moving on the bridge. Numerical simulation show that the method is effective and the damage location can be determined accurately.

The following conclusions can be drawn from the results:

- (1) The crack location is determined as the position of the maximum value in the wavelet coefficient curve and there is no baseline requirement in determining the damage location. The damage extent can be determined using a reference database of the damage index based on the wavelet coefficient.
- (2) The changes of parameters, such as load moving speed, unsprung- and sprung-mass, spring stiffness and damping, do not affect the identified position of crack in the beam.
- (3) The frequencies of the beam change obviously when the crack occurs at the location where the absolute value of mode shape is high, while change less obviously when the crack occurs at the stationary point of mode shape.
- (4) The frequencies do not change much when the crack is not deep: when the crack depth ratio reaches 30%, the first four frequencies all decreased by 2.3% at most, and the low order frequencies change more obviously than the higher order ones.

## Acknowledgements

The research of this project is supported by the Natural Science Foundation of China (51078029), the Fundamental Research Funds for the Central Universities (2009JBM078), and the Flander (Belgium)-China Bilateral Project (BIL 07/07).

## References

Bammios, Y., Douka E. and Trochidis, A. (2002), "Crack identification in beam structures using FEM", *J. Sound*

- Vib.*, **256**(2), 287-297.
- Bilello, C. and Bergman, L.A. (2004), "Vibration of damaged beams under a moving mass: theory and experimental validation", *J. Sound Vib.*, **274**, 567-582.
- Daubechies, I. (1992), *Ten lectures on wavelets, CBMS-NSF regional conference series in applied mathematics*, Society for Industrial and Applied Mathematics, Philadelphia.
- Doebling, S.W., Farrar, C.R. and Prime, M.B. (1998), "A summary review of vibration-based damage identification methods", *Shock Vib. Digest*, **30**(2), 91-105.
- Douka, E., Loutridis, S. and Trochidis, A. (2003), "Crack identification in beams using wavelet analysis", *Int. J. Solids Struct.*, **40**, 3557-3569.
- Gentile, A. and Messina, A. (2003), "On the continuous wavelet transforms applied to discrete vibrational data for detecting open cracks in damaged beams", *Int. J. Solids Struct.*, **40**, 295-315.
- Han, J.G., Ren, W.X. and Sun, Z.S. (2005), "Wavelet packet based damage identification of beam structures", *Int. J. Solids Struct.*, **42**, 6610-6627.
- Hong, J.C., Kim, Y.Y., Lee, H.C. and Lee, Y.W. (2002), "Damage detection using the Lipschitz exponent estimated by the wavelet transform applications to vibration modes of a beam", *Int. J. Solids Struct.*, **39**, 1803-1816.
- Loutridis, S., Douka, E., Hadjileontiadis, L.J. and Trochidis, A. (2005), "A two-dimensional wavelet transform for detection of cracks in plates", *Eng. Struct.*, **27**, 1327-1338.
- Mahmoud, M.A. and Abou Zaid, M.A. (2002), "Dynamic response of a beam with a crack subject to a moving mass", *J. Sound Vib.*, **256**(4), 591-603.
- Mallat, S. and Hwang, W.L. (1992), "Singularity detection and processing with wavelets", *IEEE T. Inform. Theory*, **38**(2), 617-643.
- Masoud, S., Jarrah, M.A. and Maamory, M.A. (1998), "Effect of crack depth on the natural frequency of a prestressed fixed-fixed beam", *J. Sound Vib.*, **214**(2), 201-212.
- Montalvão, D., Maia, N.M.M. and Ribeiro, A.M.R. (2006), "A review of vibration-based structural health monitoring with special emphasis on composite materials", *Shock Vib. Digest*, **38**(4), 1-30.
- Narkis, Y. (1994), "Identification of crack location in vibrating simply-supported beams", *J. Sound Vib.*, **172**(4), 549-558.
- Narkis, Y. and Elmalah, E. (1996), "Crack identification in a cantilever beam under uncertain end condition", *J. Mech. Sci.*, **38**(5), 499-507.
- Philips, P. (2009), "A quasistatic crack propagation model allowing for cohesive forces and crack reversibility", *Interact. Multiscale Mech.*, **2**(1), 31-44.
- Salawu, O.S. (1997), "Detection of structural damage through changes in frequency: a review", *Eng. Struct.*, **19**(9), 718-723.
- Sinha, J.K., Friswell, M.I. and Edwards, S. (2002), "Simplified models for the location of cracks in beam structures using measured", *J. Sound Vib.*, **251**(1), 13-38.
- Staszecski, W.J. (1998), "Structural and mechanical damage detection using wavelets", *Shock Vib. Digest*, **30**(6), 457-472.
- Tada, H., Paris, P. and Irwin, G. (1973), *The stress analysis of cracks handbook*, Hellertown, Pennsylvania: Del Research Corporation.
- Xiang, Z.H. and Zhang, Y. (2009), "Changes of modal properties of simply-supported plane beams due to damages", *Interact. Multiscale Mech.*, **2**(2), 153-175.
- Yuen, M.M.F. (1985), "A numerical study of the eigen parameters of a damaged cantilever beam", *J. Sound Vib.*, **103**, 301-310.
- Zhu, X.Q. and Law, S.S. (2006), "Wavelet-based crack identification of bridge beam from operational deflection time history", *Int. J. Solids Struct.*, **43**, 2299-2317.